Molecular Therapy
Oncolytics
Original Article

Ligand-based, piggyBac-engineered CAR-T cells targeting EGFR are safe and effective against non-small cell lung cancers

Thanyavi Chinsuwan,[1,2] Koichi Hirabayashi,[1] Shuji Mishima,[3] Aiko Hasegawa,[1] Miyuki Tanaka,[1,4] Hidemi Mochizuki,[4,5] Akihito Shimoi,[4,5] Takashi Murakami,[6] Shigeki Yagyu,[1,4] Kimihiro Shimizu,[3] and Yozo Nakazawa[1,4,7]

[1]Department of Pediatrics, Shinshu University School of Medicine, Matsumoto, Nagano, Japan; [2]Department of Microbiology, Faculty of Medicine, Chulalongkorn University, Bangkok, Thailand; [3]Division of General Thoracic Surgery, Department of Surgery, Shinshu University School of Medicine, Matsumoto, Nagano, Japan; [4]Center for Advanced Research of Gene and Cell Therapy, Shinshu University School of Medicine, Matsumoto, Nagano, Japan; [5]Ina Research Inc., Ina, Nagano, Japan; [6]Department of Microbiology, Faculty of Medicine, Saitama Medical University, Iruma, Saitama, Japan; [7]Institute for Biomedical Sciences, Interdisciplinary Cluster for Cutting Edge Research, Shinshu University, Matsumoto, Nagano, Japan

Epidermal growth factor receptor (EGFR) is overexpressed in various cancers, including non-small cell lung cancer (NSCLC), and in some somatic cells at a limited level, rendering it an attractive antitumor target. In this study, we engineered chimeric antigen receptor (CAR)-T cells using the piggyBac transposon system, autologous artificial antigen-presenting cells, and natural ligands of EGFR. We showed that this approach yielded CAR-T cells with favorable phenotypes and CAR positivity. They exhibited potent antitumor activity against NSCLC both *in vitro* and *in vivo*. When administered to tumor-bearing mice and non-tumor-bearing cynomolgus macaques, they did not elicit toxicity despite their cross-reactivity to both murine and simian EGFRs. In total we tested three ligands and found that the CAR candidate with the highest affinity consistently displayed greater potency without adverse events. Taken together, our results demonstrate the feasibility and safety of targeting EGFR-expressing NSCLCs using ligand-based, piggyBac-engineered CAR-T cells. Our data also show that lowering the affinity of CAR molecules is not always beneficial.

INTRODUCTION

Epidermal growth factor receptor (EGFR) is a receptor tyrosine kinase in the ErbB receptor family. Overexpression, mutation, or dysregulation of this receptor, leading to excessive growth signals, are the hallmarks of several solid tumors, including non-small cell lung cancer (NSCLC). Therefore, targeting this receptor/ligand axis is an attractive antitumor strategy. For immunotherapeutic strategies, four anti-EGFR monoclonal antibodies (mAbs) have been approved for treating various cancers of epithelial origin.[1]

In the past two decades, an emerging form of adoptive cellular therapy termed "chimeric antigen receptor" (CAR) has shown unprecedented results in treating B cell malignancies.[2] CAR is a synthetic fusion protein composed of an antigen-binding extracellular domain, canonically a single-chain variable fragment (scFv) of an antibody, fused to one or two T cell costimulatory domains and terminally to T cell intracellular signaling domain CD3ζ. Most clinical trials and all approved CAR therapies utilize T cells that are inserted with a CAR transgene (CAR-T). Despite encouraging response rates in hematologic malignancies, CAR-T therapies remain largely ineffective when tested against various solid malignancies.[3]

To manufacture CAR-Ts, autologous T cells are typically activated with anti-CD3 and anti-CD28 mAbs before being transduced with lentivirus or retrovirus.[4] While this reliably yields multifold cell expansion and a high proportion of CAR^+ cells, rigorous quality control is also required to ensure that no replication-competent virus remains in the final product, increasing production complexity and cost.[4] Depending on the duration of contact with mAbs, excessive stimulation could also lead to terminal differentiation and, thus, poor persistence of CAR-Ts.[5] Both of these can be avoided with transposon-based manufacturing protocols, which circumvent the need to check for replication-competent viruses. Furthermore, they do not require T cell pre-activation and yield more cells with memory phenotypes.[6,7] Cells with favorable memory phenotypes are associated with durable remissions in recipients of CAR-T treatments with hematologic malignancies.[8] It is reasonable to presume that these cells will also be an invaluable component as we advance CAR-Ts to tackle solid tumors. To date, piggyBac and Sleeping Beauty are the two

Received 16 February 2023; accepted 14 September 2023;
https://doi.org/10.1016/j.omto.2023.100728.

Correspondence: Koichi Hirabayashi, MD, PhD, Department of Pediatrics, Shinshu University School of Medicine, Matsumoto, Nagano, Japan.
E-mail: kohira@shinshu-u.ac.jp
Correspondence: Yozo Nakazawa, MD, PhD, Department of Pediatrics, Shinshu University School of Medicine, Matsumoto, Nagano, Japan.
E-mail: yxnakaza@shinshu-u.ac.jp

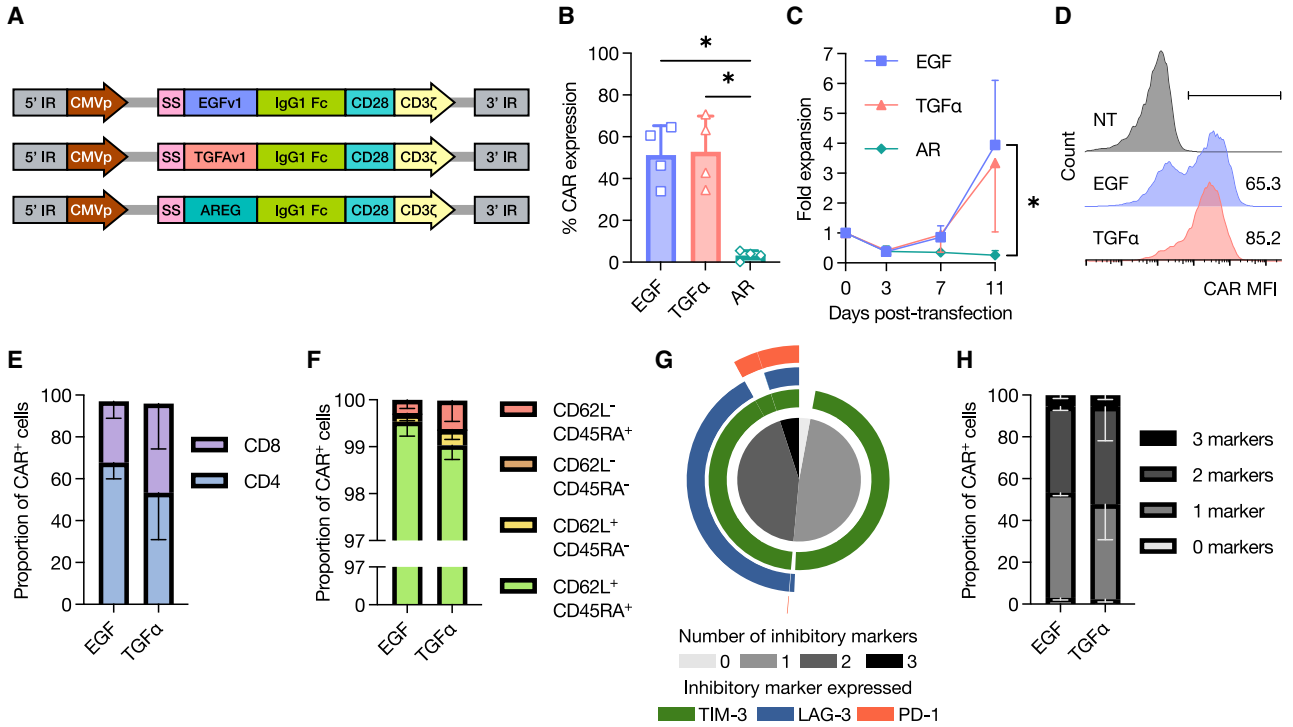

Figure 1. Two out of three anti-EGFR CAR constructs were successfully expressed and expanded with favorable phenotypes

(A) Anti-EGFR CAR plasmids were created by replacing the FMC63 scFv sequence of pIRII-CAR.CD19-28ζ with those of natural ligands that are specific to EGFR: EGF, TGF-α, and AR. IR, inverted repeats; CMVp, CMV immediate-early promoter/enhancer; SS, signal sequence; IgG1 Fc, fragment crystallizable region of human IgG1. (B and C) Percentage of CAR expression on the surface of transfected cells 12 days post transfection (B) and fold expansion of each CAR construct at the specified time points (C). Statistical significance was determined using unpaired t test. n = 4. *$p < 0.05$. (D) Representative histograms showing cell-surface density of transfected CAR. (E) Proportions of $CD4^+$ and $CD8^+$ cells among CAR^+ cells. n = 3. (F) Memory phenotypes of CAR^+ cells as quantified by surface expression of CD62L and CD45RA. n = 3. (G) Representative diagram showing the expression of three different inhibitory markers on the CAR^+ product prior to downstream experiments. TIM-3, T cell immunoglobulin and mucin domain-containing protein 3; LAG-3, lymphocyte activation gene-3; PD-1, programmed cell death protein 1. (H) Proportions of CAR^+ cells expressing 0, 1, 2, or 3 inhibitory markers. n = 3. All data are shown as mean ± SD.

transposon systems that have been clinically validated for manufacturing CAR-T products.[9]

The antigen-recognition motifs of most CARs are derived from scFvs. Recent developments, however, have experimented with other moieties, including natural ligand/receptor pairings.[10] While scFvs offer the flexibility of targeting any surface antigen with a corresponding mAb, they may also entail pitfalls, such as domain swapping, tonic signaling, unfolding due to hydrophobic residues, and potential immunogenicity.[11] On the other hand, natural ligand/receptor pairings can bypass these constraints and facilitate rapid pre-clinical development with low risk of immunogenicity.[11]

One particular CAR-T product targeting EGFR has been tested in phase I clinical trials, with no deaths and few reversible grade 3/4 adverse events.[12–14] Several other pre-clinical developments have also been published.[15–17] Most of the candidates published so far are scFv CARs integrated via viral transduction, with some notable exceptions.[18–20] In this study, we present the development of the first ligand-based, piggyBac-transfected anti-EGFR CARs, using NSCLC as a model target.

RESULTS

EGF-CAR and TGFα-CAR were expressed and expanded effectively

To construct ligand-based EGFR-specific CARs, we selected three ligands that bind exclusively to EGFR and span three orders of magnitude of affinity toward the receptor: epidermal growth factor (EGF), transforming growth factor α (TGF-α), and amphiregulin (AR).[21,22] We used pIRII-CAR.CD19-28ζ as the backbone for all three constructs,[23] replacing anti-CD19 scFv with EGFR ligands (Figure 1A). The CAR-T products generated from these plasmids were named EGF-CAR, TGFα-CAR, and AR-CAR, respectively. Using the artificial feeder protocol for expansion described earlier,[24] EGF-CAR and TGFα-CAR were reliably expressed and expanded, while AR-CAR failed at both (Figures 1B and 1C). Based on this, we proceeded with EGF-CAR and TGFα-CAR.

Table 1. Specific antibody-binding capacity (SABC) of each cell line

Cell line	Cell type	SABC ($\times 10^3$)
HCC827-Luc	NSCLC (adenocarcinoma)	272.5 ± 30.9
NCI-H1975-Luc	NSCLC (adenocarcinoma)	38.9 ± 7.8
A549-Luc	NSCLC (adenocarcinoma)	40.8 ± 12.3
RERF-LC-Sq1/CMV-Luc	NSCLC (squamous cell carcinoma)	116.4 ± 10.3
NCI-H460-Luc	NSCLC (large cell carcinoma)	29.6 ± 3.7
A431	Epidermoid carcinoma (skin)	551.4 ± 51.6
K562	CML in blast crisis	0.0

NSCLC = non-small cell lung cancer. CML = chronic myeloid leukemia. SABC values are presented as mean ± SD.

Next, we characterized the phenotypes of the two CAR constructs. As expected from cytomegalovirus (CMV) promoter and piggyBac transposase, the cell-surface densities of CAR polypeptides were moderate (Figure 1D). The CD4/CD8 ratios were similar ($p = 0.13$, unpaired t test) and were not skewed toward one cell type (Figure 1E). Memory phenotypes of both CARs were exceptionally favorable, with over 99% of CAR^+ cells expressing both CD45RA and CD62L (Figure 1F), implying that they were either naive or stem cell-like memory T cells.[25] Prior to downstream experiments, almost all CAR^+ cells expressed T cell immunoglobulin and mucin domain-containing protein 3 (TIM-3), approximately half expressed lymphocyte activation gene 3 (LAG-3), and only a few expressed programmed cell death protein 1 (PD-1) (Figures 1G and 1H). These characteristics are consistent with previous reports of piggyBac-engineered CAR-T cells.[26] To determine whether tonic signaling was responsible for TIM-3 and LAG-3 expression, we compared the forward scatter and expression of CD25 and CD69 between activated T cells (ATCs), CD19-CAR, and EGF-CAR (Figure S1). We found no difference between our EGF-CAR, FMC63-based CD19-CAR, which lacks tonic signaling,[27,28] and ATCs, which were stimulated by CD3/CD28 beads for 48 h on days 1 and 2 and rested. We also measured the concentration of any "leaky" interleukin-2 (IL-2) and interferon-γ (IFN-γ) in the absence of target cells; they were undetectable ($n = 5$, data not shown).

Both EGF-CAR and TGFα-CAR exhibited cytotoxicity against various NSCLC cell lines *in vitro*

For this study, we selected five NSCLC cell lines representing three main histological subtypes: large cell carcinoma (NCI-H460-Luc), squamous cell carcinoma (RERF-LC-Sq1/CMV-Luc), and adenocarcinoma. For adenocarcinoma, we chose A549-Luc, HCC827-Luc, and NCI-H1975-Luc whose EGFRs are wild-type, harbor del746-750, and harbor L858R/T790M double mutations, respectively. Del746-750 in exon 19 and L858R substitution in exon 21 render an NSCLC hypersensitive to tyrosine kinase inhibitors (TKIs), while T790M substitution confers resistance.

To gauge how effective EGF-CAR and TGFα-CAR could be against these NSCLC cell lines, we first quantified the expression of EGFR in each of them. We found that A549-Luc, NCI-H1975-Luc, and NCI-H460-Luc cells expressed similar EGFR levels at approximately 30–40 $\times 10^3$ receptors/cell; RERF-LC-Sq1/CMV-Luc expression was approximately three times higher, while HCC827-Luc expression was six times greater than these three cell lines (Table 1).

Both CARs exhibited considerable cytotoxicity against A549-Luc, NCI-H1975-Luc, and HCC827-Luc cell lines when compared to ATCs across all tested effector/target (E/T) ratios (Figure 2A). Cytotoxicity was corroborated by the concentrations of IL-2 and IFN-γ in the supernatant (Figure 2B). However, neither cytokine secreted by TGFα-CAR differed from ATCs for any target, despite the clear cytotoxicity of TGFα-CAR against all three target cells. On the contrary, those secreted by EGF-CAR were higher than those of both effectors and achieved statistical significance for all targets. Notably, IL-2 and IFN-γ concentrations positively correlated with EGFR density on target cells, with concentrations being the highest when tested against the HCC827-Luc cell line. From these experiments, we found that EGF-CAR was more potent than TGFα-CAR in all NSCLC cell lines examined. To complement these results from adenocarcinoma subtype, we confirmed the cytotoxicity of EGF-CAR against RERF-LC-Sq1/CMV-Luc and H460-Luc (Figure S2A). We also tested EGF-CAR against EGFR-negative Raji and, reassuringly, no off-target cytotoxicity was observed (Figure S2B). Taken together, we showed that CAR-Ts based on ligands of EGFR were capable of specifically lysing EGFR-expressing NSCLC cell lines of all three subtypes and that their cytotoxicity depended on EGFR density on target cells.

EGF-CAR was functionally superior to Cetux-CAR *in vitro*

Next, we contextualized the ligand-based CARs against a more conventional scFv-based CAR. We selected cetuximab because it is an archetypal anti-EGFR antibody and because CAR-Ts based on it have undergone prior testing.[15,17,19,20] The comparator CAR based on cetuximab (Cetux-CAR) is identical to every construct in our study except the antigen-recognition domain (Figure S3A).

Following identical manufacturing procedures and readout methods, the CAR positivity, cell expansion, memory phenotype, exhaustion markers, and activation markers between ligand-based CARs and Cetux-CAR were indistinguishable (Figures S3B–S3F). Functionally, one round of 72-h coculture with H460-Luc or RERF-LC-Sq1/CMV-Luc did not differentiate between EGF-CAR and Cetux-CAR (Figure S3G). Therefore, we subjected the two CARs to three rounds of sequential coculture with RERF-LC-Sq1/CMV-Luc at an initial seeding ratio of only 1:2. Both CARs performed similarly in the first round, consistent with previous attempts; however, EGF-CAR demonstrated stronger potency in the second and third rounds (Figures 3A and 3B). This finding was supported by the concentrations of secreted IFN-γ in those rounds (Figure 3C). At the end of the third round, more $CD3^+$ cells were detected in the EGF-CAR group, indicating better proliferation and persistence (Figure 3D). To corroborate this finding, we found that EGF-CAR expanded robustly upon coculture with RERF-LC-Sq1/CMV-Luc; the majority of CAR^+ cells were in the third

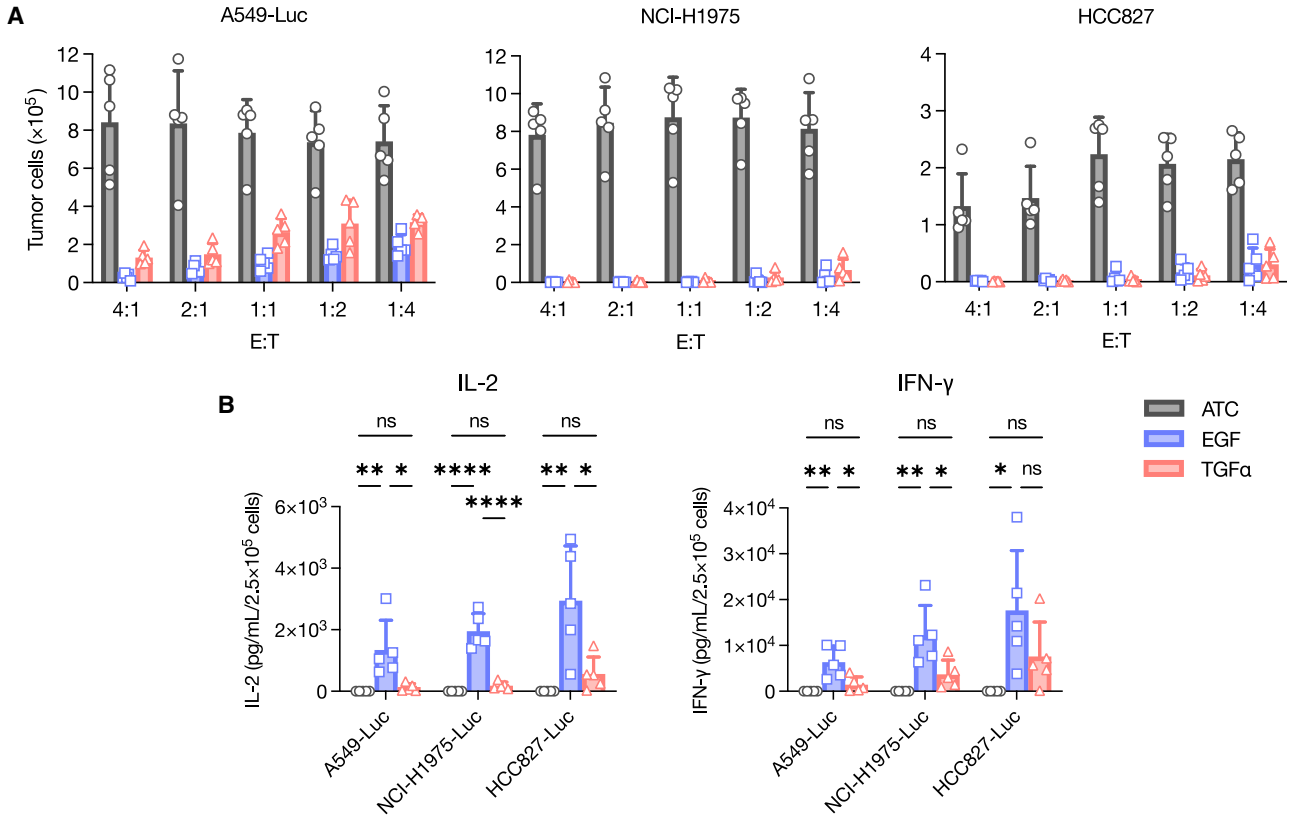

Figure 2. Both EGF-CAR and TGFα-CAR were able to effectively lyse multiple NSCLC cell lines *in vitro*, but EGF-CAR was more potent when cytokine releases were assessed

(A) *In vitro* cytotoxicity assay expressed as the number of tumor cells that remained after 5 days of coculture with activated T cells (ATC), EGF-CAR, or TGFα-CAR across a range of effector/target (E:T) ratios. n = 5. (B) IL-2 and IFN-γ concentrations in the supernatants of 1:1 coculture experiments, 24 h after the addition of effector cells. Significance was determined by one-way ANOVA with Tukey post hoc test. n = 5. *p < 0.05, **p < 0.01, ***p < 0.001, ****p < 0.0001, ns = not significant. All data are shown as mean ± SD.

generation after 72 h of coculture (Figure 3E). Exhaustion markers after the third round did not differ between the two (Figure 3F).

The comparison of TIM-3, a marker generally regarded as inhibitory, before and after the experiment is noteworthy.[29] At the end of the coculture assay, PD-1 expression on CAR$^+$ cells increased, as expected, while that of TIM-3 actually decreased (Figure 3F). This phenomenon was previously demonstrated by our group,[26] which implies that, unlike PD-1, TIM-3 expression in isolation does not always indicate a dysfunctional state of T cells.

PVAQ.EGF-CAR potently inhibited NSCLC cell line growth *in vivo*

Prior to *in vivo* experiments, we first modified the immunoglobulin 1 (IgG1) spacer in our constructs in order to abrogate its interaction with Fcγ receptors, which leads to sequestration in the lungs and activation-induced cell death.[30–33] To accomplish this, we replaced the amino acids ELLG (amino acids [aa] 233–236) and N (aa 297) in the CH_2 region with PVA and Q, respectively (Figure S4A). We verified that these mutations did not affect CAR positivity, *ex vivo* expansion, or cytotoxicity of the final product (Figures S4B–S4D). Hereafter, these CARs with mutated spacer regions are denoted with the prefix PVAQ.

We selected HCC827-Luc as the first xenograft model for evaluation because of its high EGFR expression. For this experiment, 2.5 × 10^6 HCC827-Luc cells were injected into the right flank of NOD.Cg-Prkdc^{scid}Il2rg^{tm1Wjl}/SzJ (NSG) mice. Seven days later, the mice were administered 2.0 × 10^6 CAR$^+$ cells of CD19-CAR, PVAQ.EGF-CAR, or PVAQ.TGFα-CAR via tail vein injection. Thereafter, tumor burden was monitored weekly using bioluminescence imaging (BLI) (Figure S5A). Although PVAQ.EGF-CAR rejected tumor almost to the limit of detection in four out of five mice, the tumor also failed to proliferate in three out of five mice in the CD19-CAR group (Figures S5B and S5C). The failure to proliferate was likely due to the susceptible nature of the cell line; coculture with ATCs greatly impacted the growth of HCC827-Luc *in vitro* compared to the tumor-only control (data not shown). This finding rendered the experiment inappropriate to fully evaluate the antitumor effect

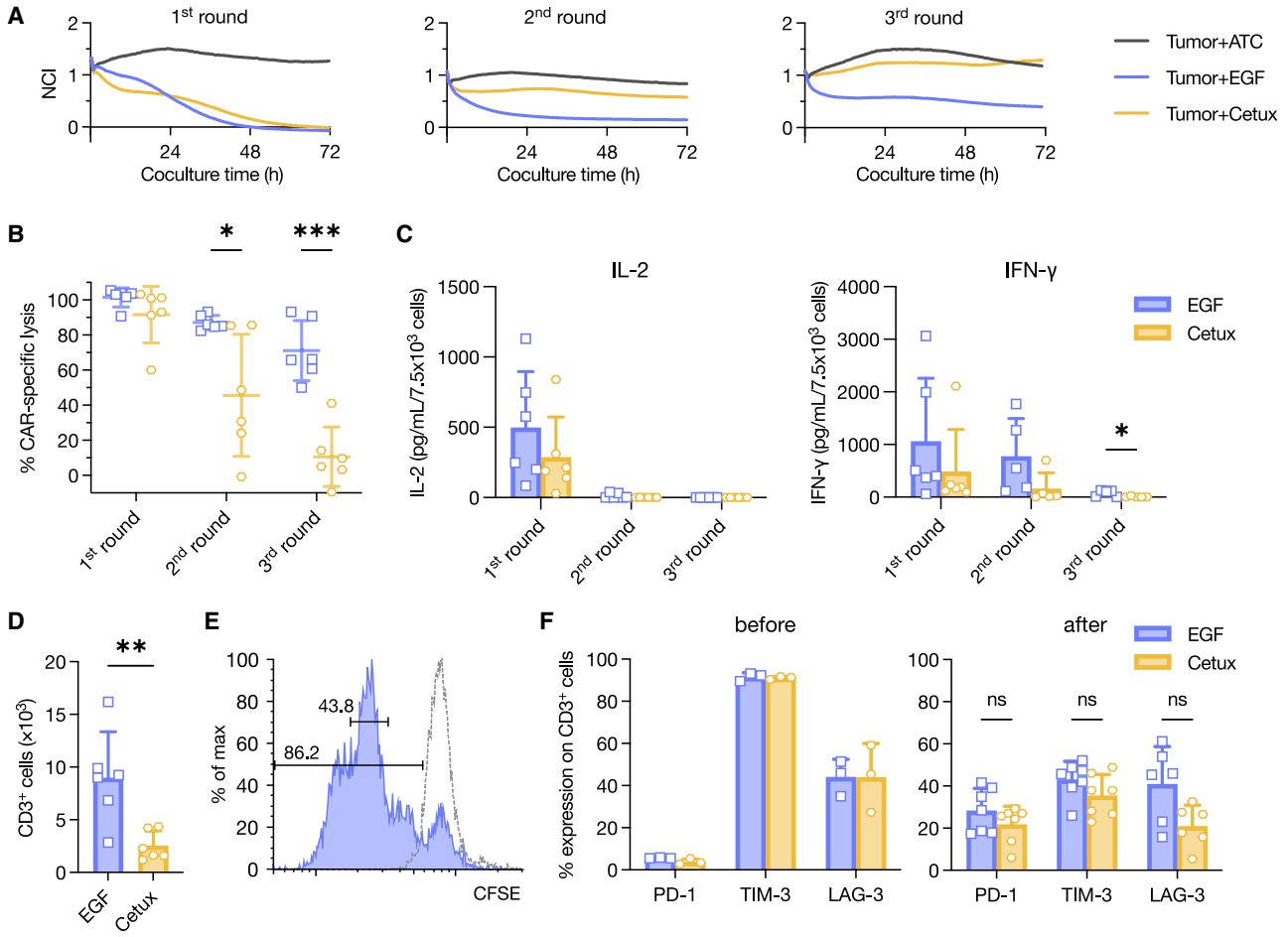

Figure 3. Sequential coculture assay revealed better potency and persistency of EGF-CAR compared to Cetux-CAR

(A and B) Sequential coculture assay of EGF-CAR against RERF-LC-Sq1/CMV-Luc using the xCELLigence Real-Time Cell Analysis system. At the end of each round, the effectors were collected and moved to the next round. Data are presented as representative plots (A) and summary showing percentage of CAR-specific lysis at the end of each round (B). n = 6. NCI, normalized cell index. (C) IL-2 and IFN-γ concentrations in the supernatants from each round, 24 h after the addition of effector cells. n = 6. (D) At the end of the third round, the remaining T cells were enumerated. One data point is the average of triplicates. n = 6. (E) Carboxyfluorescein succinimidyl ester (CFSE) staining was used to track the proliferation of EGF-CAR after 72 h of coculture with RERF-LC-Sq1/CMV-Luc. The dashed line represents unstimulated EGF-CAR from the same batch. (F) PD-1, LAG-3, and TIM-3 were quantified before the coculture and after the third round. n = 3 (before); n = 6–7 (after). The differences between EGF-CAR and Cetux-CAR were compared with multiple unpaired t tests with Holm-Šídák correction (B, C, and F) or unpaired t test (D). *p < 0.05, **p < 0.01, ***p < 0.001; ns, not significant. All data are shown as mean ± SD.

of our anti-EGFR CARs, and we euthanized all mice on day 63. We analyzed peripheral blood, bone marrow, and spleen of all 15 mice and found that PVAQ.EGF-CAR readily proliferated and persisted, in line with the tumor flux data (Figures S5D–S5F).

Consequently, we examined another xenograft model, NCI-H1975-Luc. We slightly increased the initial number of injected tumor cells to 3.0×10^6 cells while retaining the number of CAR-Ts at 2.0×10^6 cells. The rest of the procedure remained the same (Figure S5A). In this study, we found that both PVAQ.TGFα-CAR and PVAQ.EGF-CAR exerted superior tumor control over CD19-CAR (Figures 4A and 4B). In accordance with previous *in vitro* experiments, PVAQ.EGF-CAR demonstrated stronger antitumor potency and conferred significant survival benefits compared to PVAQ.TGFα-CAR (data not shown). On day 24, when we sacrificed four out of five mice in control group, we drew peripheral blood from all 15 mice and evaluated the persistence of CAR-T cells (Figure 4C). Similar to the HCC827-Luc model, PVAQ.EGF-CAR was detected at the largest number which was significantly higher than those in the other two groups (Figure 4D).

In both the HCC827-Luc and NCI-H1975-Luc xenograft experiments, no mice died unless their tumors became overbearing. From CAR infusion to the point where they succumbed to tumor burden or were sacrificed, the mice had a normal coat, normal appearance, unchanged appetite, and energetic behavior. Since human EGF can

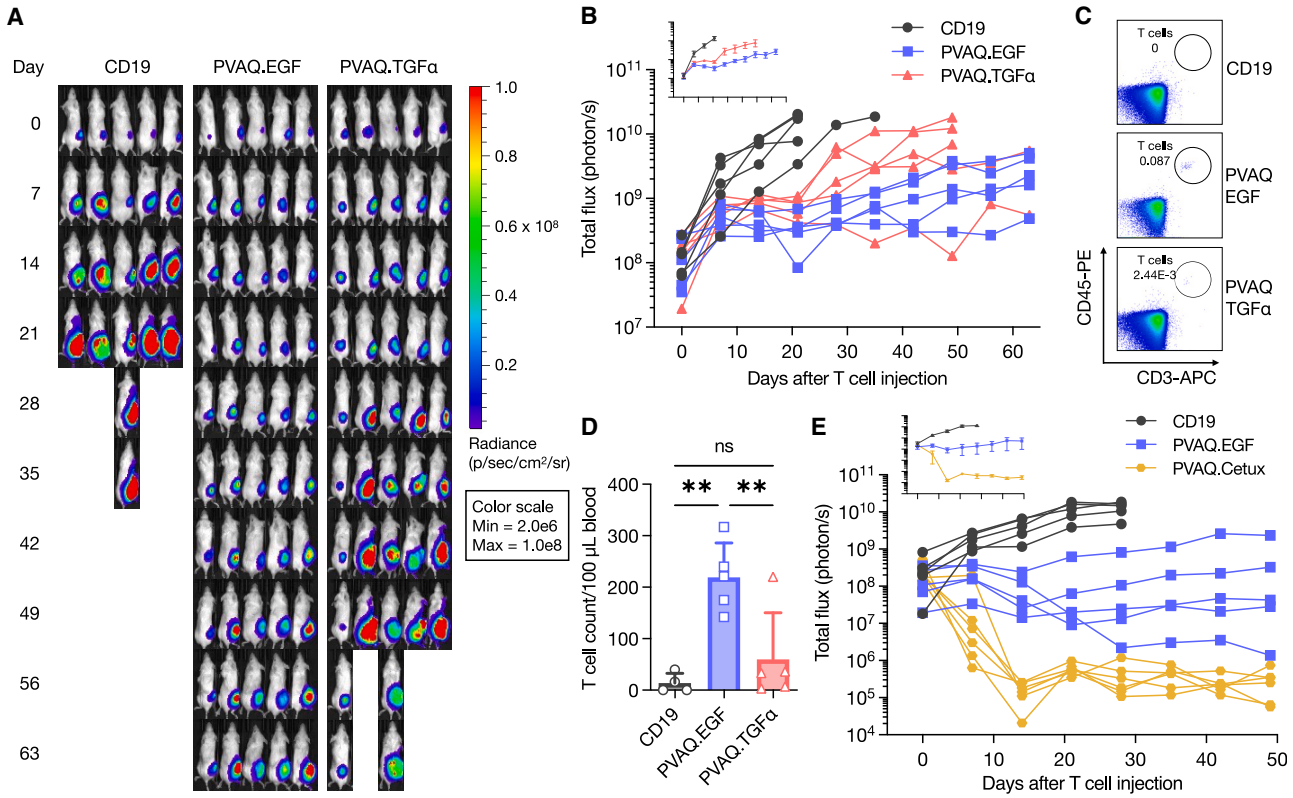

Figure 4. PVAQ.EGF-CAR exhibited significant antitumor effects *in vivo*

(A and B) Serial BLI was used to assess the size (A) and relative growth (B) of the grafted H1975-Luc tumor over time in each mouse (n = 5 per group). The tiny graph on the top left corner of (B) shows the summary data, presented as mean ± SEM. (C and D) On day 24, when four out of five mice in the control group were euthanized, blood samples were drawn from all mice, and the presence of infused CAR-T products were quantified by gating for $CD45^{+}CD3^{+}$ cells in peripheral blood (C). Summary data are presented as mean ± SD (D). Significance was determined by one-way ANOVA with Tukey post hoc test. $^{**}p < 0.01$; ns, not significant. (E) The same xenograft model was repeated to assess the potency of PVAQ.EGF-CAR against PVAQ.Cetux-CAR.

bind to murine EGFR with an affinity that is even stronger than that of human EGFR,[34] this is pertinent to the safety concerns of targeting EGFR, which is a tumor-associated antigen.[35] These results demonstrate the potency without overt toxicity of PVAQ.EGF-CAR against NSCLC murine xenograft models.

Finally, we repeated the NCI-H1975-Luc experiment to compare PVAQ.EGF-CAR and PVAQ.Cetux-CAR. In contrast to *in vitro* experiments, PVAQ.Cetux-CAR displayed stronger tumor suppression *in vivo* (Figure 4E).

Administration of ligand-based anti-EGFR CARs into non-human primates was safe

Although the safety profile of our anti-EGFR CARs from murine experiments appears promising, extrapolating this result to human settings warrants caution. Despite cross-reactivity, other factors including differences in antigen expression patterns, tissue microenvironments, and anatomical barriers could still confound the apparent lack of on-target/off-tumor toxicity in mice.[36] To verify the safety of CAR-T products, we have previously established non-human primate (NHP) models to better recapitulate human physiology using lymphodepleted cynomolgus macaques (*Macaca fascicularis*).[37,38]

We first examined the similarities between human and cynomolgus macaque EGFR, EGF, and TGF-α proteins. Using the BLAST (Basic Local Alignment Search Tool), the extracellular portion of EGFR and the mature forms of EGF and TGF-α were 99.4%, 98.1%, and 100% positive, respectively. (RefSeq: NP_005219.2 vs. XP_005549616.1; NP_001954.2 vs. XP_005555736.2; NP_003227.1 vs. XP_045225063.1, respectively). In the case of EGF ligand, only one out of 53 amino acids did not match, but evidence shows that human EGF can act as an active compound when maturing immature oocytes of cynomolgus macaques[39] and that it can accelerate corneal wound healing in tested cynomolgus macaques,[40] indicating cross-reactivity. Based on this, we reasoned that cynomolgus macaques would be a feasible NHP model for evaluating the toxicity of our anti-EGFR CARs.

As previously described,[37,38] we lymphodepleted five non-tumor-bearing macaques using cyclophosphamide and fludarabine (Figure 5A). Prior to CAR-T infusion, lymphoid cells were successfully

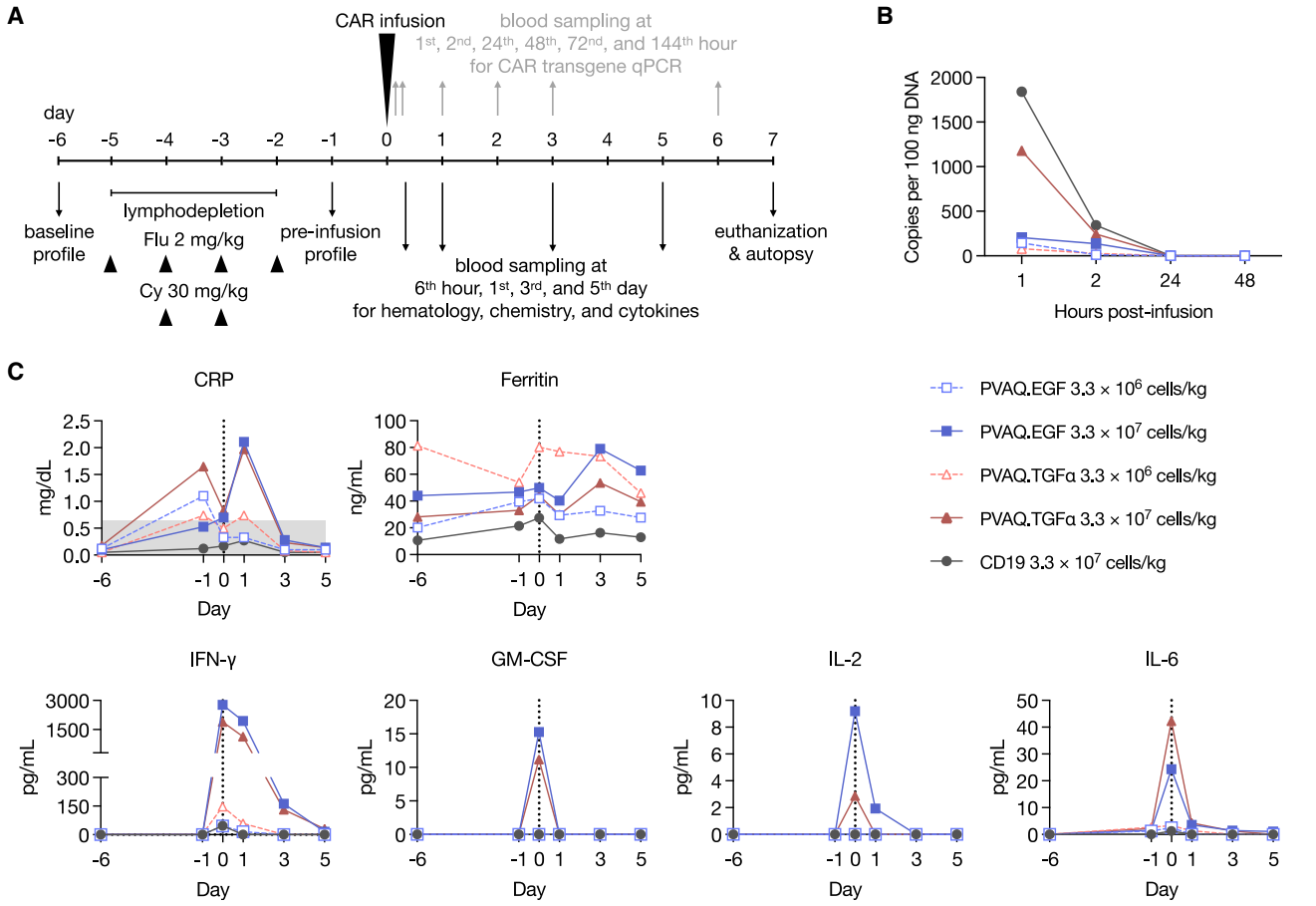

Figure 5. Anti-EGFR CAR administration was safe in lymphodepleted cynomolgus macaques at clinically relevant doses

(A) Overview of the experiment timeline. Flu, fludarabine; Cy, cyclophosphamide. (B) CAR transgene copies per 100 ng of extracted DNA from peripheral blood over time. (C) The amount of C-reactive protein (CRP), ferritin, and selected pro-inflammatory cytokines. IL-1β and TNF-α were undetectable in all subjects at all time points and therefore are not shown. Day 0 denotes 6 h after infusion. Gray band denotes normal limits established from in-house data collection. Dotted vertical line delineates pre- and post-infusion period. IFN-γ, interferon-γ; GM-CSF, granulocyte-macrophage colony-stimulating factor; IL, interleukin.

suppressed with retention of the myeloid compartment; both effects persisted until the end of the experiment (Figure S6A).

On day 0, each macaque was administered 3.3×10^6 or 3.3×10^7 total cells/kg of PVAQ.EGF-CAR or PVAQ.TGFα-CAR. As a control, one macaque was administered 3.3×10^7 total cells/kg of CD19-CAR. When adjusted for CAR$^+$ proportions, the doses became 1.5×10^6 (10^7), 1.8×10^6 (10^7), and 1.0×10^7 cells/kg for PVAQ.EGF-CAR, PVAQ.TGFα-CAR, and CD19-CAR, respectively (Figure S6B). For anti-EGFR CARs, the lower doses are in accordance with phase I clinical trials,[12–14] while the 10-fold higher doses are higher than in any clinical report thus far.

After CAR-T infusion, no test subjects showed any clinical signs of abnormality, even in those who received higher doses. There were also no changes in food intake or body weight compared to the pre-infusion period. Serial blood sampling revealed that copies of the CAR transgene could be detected during the first 2 h of infusion before becoming undetectable from the 24th hour onward (Figure 5B). We also monitored biochemical markers, including C-reactive protein (CRP), ferritin, and a panel of pro-inflammatory cytokines, namely IL-1β, IL-2, IL-6, IFN-γ, tumor necrosis factor α (TNF-α), and granulocyte-macrophage colony-stimulating factor (GM-CSF). At the clinically relevant doses, neither anti-EGFR CAR induced any meaningful changes in any of these markers (Figure 5C). However, at the higher doses, four out of six cytokines that were monitored, as well as CRP, showed steep increases at the 6th hour. Most of these increases returned to baseline by the 1st day or persisted as late as the 3rd day in the case of IFN-γ. This implied a transient activation of anti-EGFR CAR-T cells at the higher doses. Other biochemical markers that could implicate organ damage were either within normal limits throughout the entire experiment or elevated after lymphodepletion but before CAR infusion (Figure S6C). In the case of CD19-CAR, which utilized FMC63 scFv, non-reactivity and non-proliferation were as expected, as the scFv reportedly does not cross-react with NHP CD19.[41,42]

On day 7, all the macaques were euthanized and autopsied. Given that in anti-EGFR CAR trials most non-hematologic adverse events were found in the lungs or skin, we were particularly attentive to these two organs. Reassuringly, histological examination on them did not reveal any mononuclear cell infiltrates (Table S1, where examination of every organ is also provided). Taken together, we showed that in non-tumor-bearing, lymphodepleted cynomolgus macaques, anti-EGFR CARs did not induce acute on-target/off-tumor toxicity and did not effectively expand.

DISCUSSION

In this study, we demonstrated the feasibility of designing CAR molecules utilizing the natural ligands of EGFR to target the receptor itself. Both TGFα-CAR and EGF-CAR (and later, their modified IgG1 spacer variants) can be effectively manufactured using the piggyBac system. The final products exhibited exceptional memory and inhibitory phenotypes. EGF-CAR consistently displayed superior antitumor effects compared to TGFα-CAR and CD19-CAR both *in vitro* and *in vivo*. Using a murine xenograft NSCLC model, PVAQ.EGF-CAR provided a significant survival benefit without apparent toxicity; this lack of toxicity was also seen in the NHP model, wherein PVAQ.EGF-CAR administration at a clinically relevant dose did not proliferate or induce overt adverse events clinically, chemically, or histologically. However, we also showed that transient activation is possible at a dose 10-fold higher than this.

Unlike hematologic malignancies, tumor-specific antigens are rare when CAR therapies are used to target solid malignancies.[35] Consequently, tumor-associated antigens are often selected during the design process. As these targets are also expressed in normal tissues, caution must be taken with regard to the on-target/off-tumor toxicity of these CAR products. We were able to demonstrate the absence of overt toxicity in both murine and simian models despite firm evidence that human EGF cross-reacts with EGFR in both species.[34,39,40] However, we could not evaluate the possibility of cytokine release syndrome (CRS) or immune effector-cell associated neurotoxicity syndrome (ICANS), both of which are associated with high tumor burden,[43] because a xenograft NHP model does not exist. A humanized mouse xenograft model capable of recapitulating CRS and ICANS has been reported,[44] which provides an opportunity to overcome this limitation of our study.

Although sensitizing mutations of EGFR in NSCLCs allow some patients to benefit from TKIs, these mutations are considerably more common in adenocarcinomas, non-smokers, women, and Asian populations,[45,46] thus leaving other subgroups with unmet needs. Even worse, these EGFR-mutant NSCLCs will eventually develop resistance to TKIs via secondary mutations or amplifications of c-MET, leading to disease progression.[47] Another mode of targeting EGFR, mAbs, in combination with chemotherapy, has been shown to improve overall survival in patients with advanced squamous NSCLC but not in those with non-squamous subtypes.[48–51] Here we showed that anti-EGFR CARs were effective against NSCLC regardless of mutational status of EGFR or histological subtype. In particular, both PVAQ.EGF-CAR and PVAQ.Cetux-CAR displayed strong antitumor potency *in vivo* against H1975-Luc, which is insusceptible to first- and second-generation TKIs as well as anti-EGFR mAbs.[52,53] Therefore, these cellular products may present another line of treatment against advanced NSCLC.

Recently, there has been increasing interest in tuning the affinity of the antigen-recognition motif to optimize the therapeutic index of a CAR product and to delay its exhaustion.[54] We took this into consideration and utilized three ligands specific to EGFR: EGF and TGF-α, which have nanomolar affinities (0.6 and 9.2 nM, respectively), and AR, which has micromolar affinity (0.35 μM).[22] Our work contradicts Park et al.,[55] who tested ligand-based CAR-Ts directed at intercellular adhesion molecule 1 (ICAM-1) using several affinity variants of its natural ligand. They demonstrated that a ligand variant with micromolar affinity achieved superior antitumor efficacy and safety compared to other variants with nanomolar affinities. In our study, the micromolar candidate AR failed to express and expand. On the other hand, the candidate with the highest affinity, EGF, consistently provided better tumor control without apparent toxicity against targets with intermediate (NCI-H1975-Luc) and high (HCC827-Luc) levels of EGFR densities compared to TGF-α. Our contradictory data indicate the intricate nature of ligand/receptor pairings when exploited for CAR designs and underlines the need to verify each pairing on a case-by-case basis.

We also confirmed earlier results by Watanabe et al. that modifying the IgG1 spacer from ELLG (aa 233–236) to PVA and N (aa 297) to Q averted the CAR-Ts from entrapment and allowed them to act at the tumor site.[31] To address this issue, we also tried to replace the IgG1 Fc spacer of EGF-CAR with a CD28 spacer, which is shorter in length, but its expansion was poor and its antitumor activity was even weaker than that of TGFα-CAR (data not shown). Our data align with those of Xia et al.,[15] whose scFv-based anti-EGFR CAR-T also showed poor expansion when its spacer consisted only of the IgG1 hinge, which led them to settle their design at the full-length IgG1 Fc spacer. Both of our studies suggest that for anti-EGFR CAR designs, a longer spacer may be preferable.

Upon completion of CAR-T manufacture, very few cells expressed PD-1 but almost all cells expressed TIM-3, a curious combination that might be a cause for concern. While mounting evidence indicates that TIM-3 expression signifies dysfunctional T cells,[29] a non-trivial body of literature also suggests that such a generalized narrative is not always the case. While TIM-3 marks exhausted T cells in chronic viral infections[56–58] and cancers,[59–61] it is also expressed by acutely activated CD4 T cells,[62] which is more relevant in the context of freshly manufactured CAR-Ts. Once activated, the TIM-3$^+$ CD4 T cell fraction displayed stronger T helper 1 effector function *in vitro* compared to its TIM-3$^-$ counterpart, and adoptive transfer of both populations into naive mice showed no difference in their persistence *in vivo*, nor did TIM-3$^+$ T cells show inferior response when lymphocytic choriomeningitis virus was inoculated.[62] Whereas the exact role of TIM-3 in T cell exhaustion is not fully

understood,[63,64] its role in T cell activation has been shown to act synergistically with the pTCR-MHC complex and relay its signaling via both MEK-ERK and Akt-mTOR pathways.[65,66] Further to this, our results show that EGF-CAR with near-universal TIM-3 expression mounted robust proliferation and antitumor activity and that TIM-3^+ cells decreased after sequential coculture assays. Altogether, this indicates that the presence of TIM-3 without PD-1 is not always detrimental. We believe that the mechanism by which TIM-3 costimulates CAR-T cells warrants further study, as it explores the less recognized aspect of this non-canonical inhibitory marker.

EGF-CAR was more potent than Cetux-CAR *in vitro* but was less potent *in vivo*. Since the purported affinities of EGF and cetuximab toward EGFR are almost identical,[22,67,68] we did not anticipate major differences when we incorporated them into CAR-T designs. Based on a literature review, there is a scarcity of studies that directly compare ligand-based CAR with scFv-based CAR directed at the same target. In one study, Han et al. tested third-generation CAR-T cells based on adnectin against that based on cetuximab.[19] Despite adnectin-based CAR having a 30-fold lower affinity toward EGFR, its antitumor activity did not differ from cetuximab-based CAR, both *in vitro* and *in vivo*. In another study by Butler et al., a CAR-T comprising an engineered variant of NKp30 receptor was compared to that comprising TZ47 scFv[69]; both directed against B7H6, a stress-induced ligand, with identical affinities. Although both CARs performed identically in killing tumor cells, their cytokine secretion profiles were vastly different when tested against $B7H6^{low}$ cell lines. The authors hypothesized that this could result from different association and disassociation constants (K_A and K_D), with the engineered natural receptor having much faster on- and off-rates despite identical K_D. However, the authors did not test both CARs *in vivo*. In essence, we believe we report the first instance of *in vitro/in vivo* reversal of CAR effectiveness because of the antigen-recognition domain. We did not investigate the cause of this discrepancy, and we intend to conduct future studies.

In summary, we have successfully proposed an alternative approach to engineering cellular immunotherapy using natural ligands of EGFR, piggyBac system, and autologous artificial feeder cells instead of scFvs, lentiviral or retroviral vectors, and anti-CD3/anti-CD28 beads, respectively. The resultant products expanded and expressed satisfactory levels of CAR molecules, displayed target-specific cytotoxicity that correlated with antigen density, and did not induce overt adverse reactions in mice or cynomolgus macaques. To comprehensively elucidate the efficacy and safety of these anti-EGFR CARs, they should be tested in phase I clinical trials. Additionally, their potency in inhibiting other EGFR-expressing solid tumors and the mechanism by which they performed differently from the other scFv-based CAR should be explored in further research.

MATERIALS AND METHODS

Ethics approval and consent

This study, involving genetic engineering, was approved by the Institutional Review Board of Shinshu University (approval no. 20-046_3). Blood from healthy donors was obtained with informed consent according to the protocol approved by the Institutional Review Board of Shinshu University School of Medicine (approval no. 4816). All experiments involving live animals were performed using protocols approved by the Shinshu University School of Medicine Institutional Animal Care and Use Committee (approval no. 021066).

Cell lines and cell cultures

Human cell lines were obtained from the Japanese Collection of Research Bioresources Cell Bank (NCI-H1975-Luc, NCI-H460-Luc, HCC827-Luc, RERF-LC-Sq1/CMV-Luc, and A549-Luc) and Riken Bioresource Research Center Cell Bank (A431). The cells were maintained in standard culture conditions (37°C, 5% CO_2, humidified) and the recommended culture media. NCI-H1975-Luc, NCI-H460-Luc, HCC827-Luc, RERF-LC-Sq1/CMV-Luc, and A549-Luc cells were cultured in RPMI 1640 + GlutaMAX-I (Life Technologies, Grand Island, NY, USA) containing 10% fetal bovine serum (FBS; GE Life Sciences, South Logan, UT, USA). A431 cells were cultured in DMEM + GlutaMAX-I (Life Technologies) containing 10% FBS.

All cell lines were periodically checked for mycoplasma contamination using the EZ-PCR Mycoplasma Detection Kit (Biological Industries, Beit HaEmek, Israel) and verified as mycoplasma free.

Plasmid construction

Plasmids encoding *piggyBac* transposase (pCMV-pB) and CD19-CAR without the CH2CH3 spacer have been described previously.[70,71] Anti-EGFR CAR plasmids were based on pIRII-CAR.CD19-28ζ[23] in which the FMC63 scFv sequence was replaced with those coding for the mature EGF peptide variant 1, TGF-α peptide variant 1, and AR peptide to create pIRII-CAR.EGFR(EGFv1), pIRII-CAR.EGFR(TGFAv1), and pIRII-CAR.EGFR(AREG), respectively. The coding sequences for the mature forms of these peptides were obtained from RefSeq: NM_001963.6, NM_003236.4, and NM_001657.4.

IgG1 spacer mutations were achieved by substituting the amino acids ELLG (aa 233–236) and N (aa 297) with PVA and Q, respectively.[31] Primers for ELLG-to-PVA mutagenesis were described previously.[30] The primers used for N297Q mutagenesis were 5′-AGT ACC AGA GCA CGT ACC GTG TGG TCA GCG-3′ and 5′-GCT CCT CCC GCG GCT TTG TCT TG-3′.

Finally, the EGFR-specific artificial feeder plasmid, pIRII-tEGFR-CD80-4-1-BBL, was constructed by substituting the truncated HER2 sequence in the pIRII-tHER2-CD80-4-1-BBL plasmid[24] with that of truncated, extracellular-domain-only EGFR.

All subclonings were performed using the In-Fusion HD Cloning Kit (Takara Bio, Shiga, Japan), all mutageneses were performed using the KOD -Plus- Mutagenesis Kit (Toyobo, Osaka, Japan), and the sequences were confirmed by Sanger sequencing (Fasmac, Kanagawa, Japan).

Manufacture of CAR-T cells

CAR-T cell manufacture was based on the artificial feeder method described previously.[24] In brief, after obtaining informed consent, blood samples were obtained from healthy donors, and peripheral blood mononuclear cells (PBMCs) were isolated by density gradient centrifugation using Ficoll-Paque PLUS (GE Healthcare, Uppsala, Sweden) and SepMate tubes (STEMCELL Technologies, Vancouver, BC, Canada). Once isolated, PBMCs were washed twice using phosphate-buffered saline (PBS). Subsequently, the cells were enumerated using a standard trypan blue exclusion test and an Olympus R1 automated cell counter (Olympus, Tokyo, Japan). To transfect each CAR transgene, 20×10^6 cells were electroporated with pIRII-CAR.EGFR(EGFv1), pIRII-CAR.EGFR(TGFAv1), or pIRII-CAR.EGFR (AREG) using 7.5 μg of the corresponding CAR plasmid and 7.5 μg of the pCMV-pB plasmid. Concurrently, 20×10^6 cells were electroporated with 15 μg of pIRII-tEGFR-CD80-4-1-BBL. All electroporations were performed using a 4D Nucleofector X Unit and P3 Primary Cell Solution with pulse code FI-115 (Lonza, Basel, Switzerland). Ten minutes after electroporation, the cells were resuspended in ALyS705 medium supplemented with 5% artificial serum (both Cell Science & Technology Institute, Miyagi, Japan), 10 ng/mL IL-7, and 5 ng/mL IL-15 (both Miltenyi Biotec, Bergisch Gladbach, Germany) and incubated in an incubator under standard conditions (37°C, 5% CO_2, humidified). After 18 h, cells electroporated with pIRII-tEGFR-CD80-4-1-BBL were irradiated with UV light and added to the remaining CAR-transfected population at a ratio of 5×10^6 to 20×10^6 CAR cells. CAR-T cells were maintained in an incubator for 12–14 days before being harvested for use in downstream experiments. Half of the culture medium was replaced every 2–3 days.

Quantification of cell-surface EGFR

The specific antibody-binding capacity (SABC) of each cell line was determined using QIFIKIT (#K0078; Dako, Glostrup, Denmark), according to the manufacturer's recommendations. In brief, five populations of calibration beads with a predefined quantity of mouse mAb molecules were stained with a secondary goat antimouse Fc F(ab′)2 fluorescein isothiocyanate (FITC) conjugate (#F0479; Dako, supplied with QIFIKIT). For each cell line, 1.0×10^5 cells were stained with either mouse antihuman EGFR (clone AY13, #352902; BioLegend, San Diego, CA, USA) or mouse IgG1κ isotype control (clone MOPC-21, #400102; BioLegend) at the same saturating concentration (15 μg/mL). After 30 min, the cells were washed and stained with the same secondary antibody as the calibration beads for 45 min. The cells and beads were then washed and analyzed using a BD FACSCanto II (BD Biosciences) on the same day with the same settings. The mean fluorescent intensity of the bead populations and their antibody-binding capacity (ABC) were then log transformed and a calibration curve was obtained by fitting a linear regression. Using the calibration curve, the SABC of each cell line was calculated by subtracting the ABC of isotype-stained cells from the ABC of anti-EGFR-stained cells.

Three to four independent experiments were performed. The cells were harvested at 50%–80% confluence and at least 24 h after the latest passage. The A431 cell line was used as the upper bound control and K562 as the negative control.

Flow cytometry

Quantification of cell-surface expression of various markers was performed on a BD FACSCelesta and analyzed using FlowJo software v10.8 (both BD Biosciences). CAR expression was detected using goat antihuman IgG (H + L) FITC antibody (#109-095-003; Jackson ImmunoResearch, West Grove, PA, USA). The other antibodies used are listed in Table S2.

In vitro cytotoxicity assay

For flow-cytometry-based cytotoxicity assays, 2.5×10^5 tumor cells per well were seeded in a 24-well culture plate. Twenty-four hours later, all culture media were removed, after which CAR-T cells were resuspended in culture media preferred by tumor cells and added to the wells at different E/T ratios. In these experiments, "effectors" refer to the total cell count without normalization for CAR^+ cells. Five days after the addition of effector cells, the effector cells were collected, and the target cells were then trypsinized and collected. Next, the cell suspension was washed, filtered through 35-μm nylon mesh, and stained with anti-CD3 FITC (clone UCHT1, #300406; BioLegend) to identify effectors, anti-B7-H3 APC (clone MIH42, #351006; BioLegend) to identify targets, and 7-amino-actinomycin D (BD Biosciences) to identify dead cells. Finally, CountBright Absolute Counting Beads (Thermo Fisher Scientific, Waltham, MA, USA) were added to the suspension, and the cells were analyzed and enumerated using a BD FACSCanto II.

For assays using the xCELLigence Real-Time Cell Analysis system (Agilent, Santa Clara, CA, USA), 7.5×10^3 HCC827-Luc cells or 1.5×10^4 RERF-LC-Sq1/CMV-Luc cells were seeded in an E-Plate 16 PET (Agilent), placed on the instrument, and allowed to adhere for 24 h. At the 24^{th} hour, all culture media were removed, and effector cells were added with fresh media at the specified E/T ratios. In these experiments, "effectors" refer only to CAR^+ cells. Cocultures lasted 72 h. The impedance was recorded every 15 min, and the final time point before the addition of effector cells was selected as the normalization time point. For sequential coculture assays using this platform, at the end of each round effector cells were gently resuspended and collected, then added to the next round of coculture using fresh media where the target cells were seeded 24 h prior.

For bioluminescence-based assay, 1.0×10^5 NCI-H460 or RERF-LC-Sq1/CMV-Luc cells were seeded in a 96-well black plate with clear bottom (ViewPlate-96 Black; PerkinElmer, Waltham, MA, USA). Twenty-four hours later, all culture media were removed, after which CAR-T cells were resuspended in culture media preferred by tumor cells and added to the wells at different E/T ratios. Seventy-two hours later, D-luciferin sodium salt (OZ Biosciences, Marseille, France) was added at a final concentration of 75 μg/mL. The reaction was allowed to occur for 30 min in an incubator. Finally, a SpectraMax iD3 plate reader (Molecular Devices, San Jose, CA, USA) was used to measure the luminescence of each well. The brightness of wells with effector

was compared to that of wells with tumor only to calculate the percentage of lysed cells.

Quantification of cytokines in supernatant

Twenty-four hours after the addition of effector cells, the supernatant from 1:1 wells was collected and stored at −80°C until analysis. To determine the concentrations of IFN-γ and IL-2, the supernatants were thawed and analyzed using an enzyme-linked immunosorbent assay (ELISA). Specifically, the DuoSet ELISA Development Systems Human IFN-γ and Human IL-2 (both R&D Systems, Minneapolis, MN, USA) were used according to the manufacturer's recommendations. Each experimental sample was analyzed in duplicate. The concentrations were derived using a four-parameter logistic regression model.

Proliferation assay

Cell proliferation was assessed using the CellTrace carboxyfluorescein succinimidyl ester (CFSE) Cell Proliferation Kit (Thermo Fisher Scientific). CAR-T cells were stained in a solution containing 5 μM CFSE for 8 min at 37°C. The effector cells were then added to a 24-well plate containing 1.0×10^5 pre-seeded tumor cells at an E/T ratio of 1:1. Coculture was conducted for 72 h, after which effector cells were collected and analyzed by flow cytometry.

In vivo murine NSCLC model

Female NSG mice were purchased from Charles River Laboratories (Yokohama, Japan) and housed at the Institute of Experimental Animals, Shinshu University School of Medicine for a week or more. At the start of the experiments, the mice were 8–9 weeks old. Food and water were provided *ad libitum*. To evaluate the antitumor effect of different CAR-Ts, 2.5×10^6 HCC827-Luc cells or 3.0×10^6 H1975-Luc cells were subcutaneously grafted onto the right flank of each mouse. Seven days later, the mice were stratified to evenly distribute the tumor burden, and 2.0×10^6 CAR^+ cells in 100 μL of PBS were administered via their tail veins. Thereafter, tumor size was monitored weekly by BLI using IVIS Lumina LT (PerkinElmer) and expressed as total flux (photons/s). To quantify tumor bioluminescence, 300 μg of D-luciferin sodium salt (OZ Biosciences) was delivered intraperitoneally, and images were acquired 10 min later using Living Image Software (PerkinElmer). Mice were euthanized when they visibly showed signs of discomfort or when statistical significance was achieved in case of survival.

NHP model for off-tumor toxicity evaluation

Five male cynomolgus macaques, aged 5–7 years, were housed at Ina Research, a facility fully accredited by the Association for Assessment and Accreditation of Laboratory Animal Care International. All procedures were performed in accordance with the Act on Welfare and Management of Animals and internally established guidelines for animal experiments. The pre-conditioning regimen, sample collection, blood analysis, and detection of CAR transgene in the sample were previously described.[38] In brief, 2 mg/kg of fludarabine was administered intravenously for 4 days from days −5 to −2, and 30 mg/kg cyclophosphamide was administered for 2 days from days −4 to −3. In addition, dexamethasone, granisetron, and mesna were administered on days −4 and −3. Finally, 60 mg of cefmetazole per day was administered from days −5 to −2 as prophylaxis. Blood and serum samples were obtained from the femoral vein at several time points (Figure 4A) and analyzed as previously described. Throughout the experiment, all macaques were closely monitored for clinical presentation, general appearance, food consumption, and body weight. At the end of the study period, the animals were anesthetized by intravenous injection of thiopental and euthanized by exsanguination from the axillary and femoral arteries and veins. Subsequently, the organs were harvested, fixed with 10% formaldehyde, and stained with hematoxylin and eosin. The specimens were then interpreted by qualified pathologists.

Statistical analyses

Statistical analyses and graph presentations were performed using GraphPad Prism 9 (GraphPad Software, San Diego, CA, USA). The exact method used for each experiment is described in the figure legends. Statistical significance was defined as $p < 0.05$.

DATA AND CODE AVAILABILITY

All data generated in this study are included in this article and its supplemental information.

SUPPLEMENTAL INFORMATION

Supplemental information can be found online at https://doi.org/10.1016/j.omto.2023.100728.

ACKNOWLEDGMENTS

This study was supported by the Japan Society for the Promotion of Science Grant-in-Aid for Scientific Research (KAKENHI) nos. 20H03639 and 22K08996 and the Japan Agency for Medical Research and Development nos. 22ae0201006h0005, 22ama221312h0001, and 20ak0101048. The authors would like to thank Editage for English language editing. Graphical illustrations (graphical abstract and Figure S5A) were created using BioRender.

AUTHOR CONTRIBUTIONS

Conceptualization, T.C., S.Y., K.S., and Y.N.; methodology & investigation, T.C., K.H., S.M., M.T., H.M., and A.S.; formal analysis, T.C. and K.H.; resources, A.H., K.H., and T.M.; funding acquisition, T.M., S.Y., and Y.N.; supervision, S.Y., K.S., and Y.N.; writing – original draft & editing, T.C. and S.Y.

DECLARATION OF INTERESTS

H.M. and A.S. are employees of Ina Research, Inc.

REFERENCES

1. Cai, W.-Q., Zeng, L.-S., Wang, L.-F., Wang, Y.-Y., Cheng, J.-T., Zhang, Y., Han, Z.-W., Zhou, Y., Huang, S.-L., Wang, X.-W., et al. (2020). The latest battles between EGFR monoclonal antibodies and resistant tumor cells. Front. Oncol. *10*, 1249. https://doi.org/10.3389/fonc.2020.01249.

2. June, C.H., and Sadelain, M. (2018). Chimeric antigen receptor therapy. N. Engl. J. Med. *379*, 64–73. https://doi.org/10.1056/NEJMra1706169.

3. Umut, Ö., Gottschlich, A., Endres, S., and Kobold, S. (2021). CAR T cell therapy in solid tumors: A short review. Memo *14*, 143–149. https://doi.org/10.1007/s12254-021-00703-7.

4. Vormittag, P., Gunn, R., Ghorashian, S., and Veraitch, F.S. (2018). A guide to manufacturing CAR T cell therapies. Curr. Opin. Biotechnol. *53*, 164–181. https://doi.org/10.1016/j.copbio.2018.01.025.

5. Kagoya, Y., Nakatsugawa, M., Ochi, T., Cen, Y., Guo, T., Anczurowski, M., Saso, K., Butler, M.O., and Hirano, N. (2017). Transient stimulation expands superior anti-tumor T cells for adoptive therapy. JCI Insight *2*, e89580. https://doi.org/10.1172/jci.insight.89580.

6. Barnett, B.E., Hermanson, D.L., Smith, J.B., Wang, X., Tan, Y., Martin, C.E., Osertag, E.M., and Shedlock, D.J. (2016). piggyBacTM-produced CAR-T cells exhibit stem-cell memory phenotype. Blood *128*, 2167. https://doi.org/10.1182/blood.V128.22.2167.2167.

7. Lin, Z., Liu, X., Liu, T., Gao, H., Wang, S., Zhu, X., Rong, L., Cheng, J., Cai, Z., Xu, F., et al. (2021). Evaluation of nonviral piggyBac and lentiviral vector in functions of CD19chimeric antigen receptor T cells and their antitumor activity for CD19+ tumor cells. Front. Immunol. *12*, 802705. https://doi.org/10.3389/fimmu.2021.802705.

8. Fraietta, J.A., Lacey, S.F., Orlando, E.J., Pruteanu-Malinici, I., Gohil, M., Lundh, S., Boesteanu, A.C., Wang, Y., O'Connor, R.S., Hwang, W.-T., et al. (2018). Determinants of response and resistance to CD19 chimeric antigen receptor (CAR) T cell therapy of chronic lymphocytic leukemia. Nat. Med. *24*, 563–571. https://doi.org/10.1038/s41591-018-0010-1.

9. Moretti, A., Ponzo, M., Nicolette, C.A., Tcherepanova, I.Y., Biondi, A., and Magnani, C.F. (2022). The past, present, and future of non-viral CAR T cells. Front. Immunol. *13*, 867013. https://doi.org/10.3389/fimmu.2022.867013.

10. Hanssens, H., Meeus, F., De Veirman, K., Breckpot, K., and Devoogdt, N. (2022). The antigen-binding moiety in the driver's seat of CARs. Med. Res. Rev. *42*, 306–342. https://doi.org/10.1002/med.21818.

11. Branella, G.M., and Spencer, H.T. (2021). Natural receptor- and ligand-based chimeric antigen receptors: Strategies using natural ligands and receptors for targeted cell killing. Cells *11*, 21. https://doi.org/10.3390/cells11010021.

12. Feng, K., Guo, Y., Dai, H., Wang, Y., Li, X., Jia, H., and Han, W. (2016). Chimeric antigen receptor-modified T cells for the immunotherapy of patients with EGFR-expressing advanced relapsed/refractory non-small cell lung cancer. Sci. China Life Sci. *59*, 468–479. https://doi.org/10.1007/s11427-016-5023-8.

13. Guo, Y., Feng, K., Liu, Y., Wu, Z., Dai, H., Yang, Q., Wang, Y., Jia, H., and Han, W. (2018). Phase I study of chimeric antigen receptor–modified T cells in patients with EGFR-positive advanced biliary tract cancers. Clin. Cancer Res. *24*, 1277–1286. https://doi.org/10.1158/1078-0432.CCR-17-0432.

14. Liu, Y., Guo, Y., Wu, Z., Feng, K., Tong, C., Wang, Y., Dai, H., Shi, F., Yang, Q., and Han, W. (2020). Anti-EGFR chimeric antigen receptor-modified T cells in metastatic pancreatic carcinoma: A phase I clinical trial. Cytotherapy *22*, 573–580. https://doi.org/10.1016/j.jcyt.2020.04.088.

15. Xia, L., Zheng, Z.Z., Liu, J.Y., Chen, Y.J., Ding, J.C., Xia, N.S., Luo, W.X., and Liu, W. (2020). EGFR-targeted CAR-T cells are potent and specific in suppressing triple-negative breast cancer both in vitro and in vivo. Clin. Transl. Immunol. *9*, e01135. https://doi.org/10.1002/cti2.1135.

16. Thokala, R., Binder, Z.A., Yin, Y., Zhang, L., Zhang, J.V., Zhang, D.Y., Milone, M.C., Ming, G.-L., Song, H., and O'Rourke, D.M. (2021). High-affinity chimeric antigen receptor with cross-reactive scfv to clinically relevant EGFR oncogenic isoforms. Front. Oncol. *11*, 664236. https://doi.org/10.3389/fonc.2021.664236.

17. Li, G., Guo, J., Zheng, Y., Ding, W., Han, Z., Qin, L., Mo, W., and Luo, M. (2021). CXCR5 guides migration and tumor eradication of anti-EGFR chimeric antigen receptor T cells. Mol. Ther. Oncolytics *22*, 507–517. https://doi.org/10.1016/j.omto.2021.07.003.

18. Li, H., Huang, Y., Jiang, D.-Q., Cui, L.-Z., He, Z., Wang, C., Zhang, Z.-W., Zhu, H.-L., Ding, Y.-M., Li, L.-F., et al. (2018). Antitumor activity of EGFR-specific CAR T cells against non-small-cell lung cancer cells in vitro and in mice. Cell Death Dis. *9*, 177. https://doi.org/10.1038/s41419-017-0238-6.

19. Han, X., Cinay, G.E., Zhao, Y., Guo, Y., Zhang, X., and Wang, P. (2017). Adnectin-based design of chimeric antigen receptor for T cell engineering. Mol. Ther. *25*, 2466–2476. https://doi.org/10.1016/j.ymthe.2017.07.009.

20. Caruso, H.G., Hurton, L.V., Najjar, A., Rushworth, D., Ang, S., Olivares, S., Mi, T., Switzer, K., Singh, H., Huls, H., et al. (2015). Tuning sensitivity of CAR to EGFR density limits recognition of normal tissue while maintaining potent antitumor activity. Cancer Res. *75*, 3505–3518. https://doi.org/10.1158/0008-5472.CAN-15-0139.

21. Linggi, B., and Carpenter, G. (2006). ErbB receptors: New insights on mechanisms and biology. Trends Cell Biol. *16*, 649–656. https://doi.org/10.1016/j.tcb.2006.10.008.

22. Sanders, J.M., Wampole, M.E., Thakur, M.L., and Wickstrom, E. (2013). Molecular determinants of epidermal growth factor binding: A molecular dynamics study. PLoS One *8*, e54136. https://doi.org/10.1371/journal.pone.0054136.

23. Huye, L.E., Nakazawa, Y., Patel, M.P., Yvon, E., Sun, J., Savoldo, B., Wilson, M.H., Dotti, G., and Rooney, C.M. (2011). Combining mTor inhibitors with rapamycin-resistant T cells: A two-pronged approach to tumor elimination. Mol. Ther. *19*, 2239–2248. https://doi.org/10.1038/mt.2011.179.

24. Nakamura, K., Yagyu, S., Hirota, S., Tomida, A., Kondo, M., Shigeura, T., Hasegawa, A., Tanaka, M., and Nakazawa, Y. (2021). Autologous antigen-presenting cells efficiently expand piggyBac transposon CAR-T cells with predominant memory phenotype. Mol. Ther. Methods Clin. Dev. *21*, 315–324. https://doi.org/10.1016/j.omtm.2021.03.011.

25. Mahnke, Y.D., Brodie, T.M., Sallusto, F., Roederer, M., and Lugli, E. (2013). The who's who of T-cell differentiation: Human memory T-cell subsets. Eur. J. Immunol. *43*, 2797–2809. https://doi.org/10.1002/eji.201343751.

26. Suematsu, M., Yagyu, S., Nagao, N., Kubota, S., Shimizu, Y., Tanaka, M., Nakazawa, Y., and Imamura, T. (2022). PiggyBac transposon-mediated CD19 chimeric antigen receptor-T cells derived From CD45RA-positive peripheral blood mononuclear cells possess potent and sustained antileukemic function. Front. Immunol. *13*, 770132. https://doi.org/10.3389/fimmu.2022.770132.

27. Landoni, E., Fucá, G., Wang, J., Chirasani, V.R., Yao, Z., Dukhovlinova, E., Ferrone, S., Savoldo, B., Hong, L.K., Shou, P., et al. (2021). Modifications to the framework regions eliminate chimeric antigen receptor tonic signaling. Cancer Immunol. Res. *9*, 441–453. https://doi.org/10.1158/2326-6066.CIR-20-0451.

28. Chen, J., Qiu, S., Li, W., Wang, K., Zhang, Y., Yang, H., Liu, B., Li, G., Li, L., Chen, M., et al. (2023). Tuning charge density of chimeric antigen receptor optimizes tonic signaling and CAR-T cell fitness. Cell Res. *33*, 341–354. https://doi.org/10.1038/s41422-023-00789-0.

29. Wolf, Y., Anderson, A.C., and Kuchroo, V.K. (2020). TIM3 comes of age as an inhibitory receptor. Nat. Rev. Immunol. *20*, 173–185. https://doi.org/10.1038/s41577-019-0224-6.

30. Hombach, A., Hombach, A.A., and Abken, H. (2010). Adoptive immunotherapy with genetically engineered T cells: modification of the IgG1 Fc 'spacer' domain in the extracellular moiety of chimeric antigen receptors avoids 'off-target' activation and unintended initiation of an innate immune response. Gene Ther. *17*, 1206–1213. https://doi.org/10.1038/gt.2010.91.

31. Watanabe, N., Bajgain, P., Sukumaran, S., Ansari, S., Heslop, H.E., Rooney, C.M., Brenner, M.K., Leen, A.M., and Vera, J.F. (2016). Fine-tuning the CAR spacer improves T-cell potency. OncoImmunology *5*, e1253656. https://doi.org/10.1080/2162402X.2016.1253656.

32. Almåsbak, H., Walseng, E., Kristian, A., Myhre, M.R., Suso, E.M., Munthe, L.A., Andersen, J.T., Wang, M.Y., Kvalheim, G., Gaudernack, G., and Kyte, J.A. (2015). Inclusion of an IgG1-Fc spacer abrogates efficacy of CD19 CAR T cells in a xenograft mouse model. Gene Ther. *22*, 391–403. https://doi.org/10.1038/gt.2015.4.

33. Koski, J., Jahan, F., Luostarinen, A., Schenkwein, D., Ylä-Herttuala, S., Göös, H., Monzo, H., Ojala, P.M., Maliniemi, P., and Korhonen, M. (2022). Novel modular chimeric antigen receptor spacer for T cells derived from signal regulatory protein alpha Ig-like domains. Front. Mol. Med. *2*, 1049580. https://doi.org/10.3389/fmmed.2022.1049580.

34. Lahti, J.L., Lui, B.H., Beck, S.E., Lee, S.S., Ly, D.P., Longaker, M.T., Yang, G.P., and Cochran, J.R. (2011). Engineered epidermal growth factor mutants with faster binding on-rates correlate with enhanced receptor activation. FEBS Lett. *585*, 1135–1139. https://doi.org/10.1016/j.febslet.2011.03.044.

35. Flugel, C.L., Majzner, R.G., Krenciute, G., Dotti, G., Riddell, S.R., Wagner, D.L., and Abou-el-Enein, M. (2023). Overcoming on-target, off-tumour toxicity of CAR T cell therapy for solid tumours. Nat. Rev. Clin. Oncol. *20*, 49–62. https://doi.org/10.1038/s41571-022-00704-3.

36. Kato, D., Yaguchi, T., Iwata, T., Katoh, Y., Morii, K., Tsubota, K., Takise, Y., Tamiya, M., Kamada, H., Akiba, H., et al. (2020). GPC1 specific CAR-T cells eradicate established solid tumor without adverse effects and synergize with anti-PD-1 Ab. eLife *9*, e49392. https://doi.org/10.7554/eLife.49392.

37. Morokawa, H., Yagyu, S., Hasegawa, A., Tanaka, M., Saito, S., Mochizuki, H., Sakamoto, K., Shimoi, A., and Nakazawa, Y. (2020). Autologous non-human primate model for safety assessment of piggyBac transposon-mediated chimeric antigen receptor T cells on granulocyte–macrophage colony-stimulating factor receptor. Clin. Transl. Immunol. *9*, e1207. https://doi.org/10.1002/cti2.1207.

38. Yagyu, S., Mochizuki, H., Yamashima, K., Kubo, H., Saito, S., Tanaka, M., Sakamoto, K., Shimoi, A., and Nakazawa, Y. (2021). A lymphodepleted non-human primate model for the assessment of acute on-target and off-tumor toxicity of human chimeric antigen receptor-T cells. Clin. Transl. Immunol. *10*, e1291. https://doi.org/10.1002/cti2.1291.

39. Yamasaki, J., Okahara-Narita, J., Iwatani, C., Tsuchiya, H., Nakamura, S., Sakuragawa, N., and Torii, R. (2008). 256 effect of epidermal growth factor on in vitro maturation of cynomolgus monkey (*Macaca fascicularis*) oocytes. Reprod. Fertil. Dev. *20*, 208. https://doi.org/10.1071/RDv20n1Ab256.

40. Brightwell, J.R., Riddle, S.L., Eiferman, R.A., Valenzuela, P., Barr, P.J., Merryweather, J.P., and Schultz, G.S. (1985). Biosynthetic human EGF accelerates healing of Neodecadron-treated primate corneas. Invest. Ophthalmol. Vis. Sci. *26*, 105–110.

41. European Medical Agency (2022). Breyanzi : EPAR - Public Assessment Report (European Medical Agency).

42. Celgene (2021). 2.6.3 summary table of pharmacological studies. In Documents Regarding Breyanzi Intravenous Injection (Pharmaceuticals and Medical Devices Agency), p. 8, https://www.pmda.go.jp/regenerative_medicines/2021/R20210322001/380809000_30300FZX00002000_H100_1.pdf.

43. Morris, E.C., Neelapu, S.S., Giavridis, T., and Sadelain, M. (2022). Cytokine release syndrome and associated neurotoxicity in cancer immunotherapy. Nat. Rev. Immunol. *22*, 85–96. https://doi.org/10.1038/s41577-021-00547-6.

44. Norelli, M., Camisa, B., Barbiera, G., Falcone, L., Purevdorj, A., Genua, M., Sanvito, F., Ponzoni, M., Doglioni, C., Cristofori, P., et al. (2018). Monocyte-derived IL-1 and IL-6 are differentially required for cytokine-release syndrome and neurotoxicity due to CAR T cells. Nat. Med. *24*, 739–748. https://doi.org/10.1038/s41591-018-0036-4.

45. Ren, J.-H., He, W.-S., Yan, G.-L., Jin, M., Yang, K.-Y., and Wu, G. (2012). EGFR mutations in non-small-cell lung cancer among smokers and non-smokers: a meta-analysis. Environ. Mol. Mutagen. *53*, 78–82. https://doi.org/10.1002/em.20680.

46. Melosky, B., Kambartel, K., Häntschel, M., Bennetts, M., Nickens, D.J., Brinkmann, J., Kayser, A., Moran, M., and Cappuzzo, F. (2022). Worldwide prevalence of epidermal growth factor receptor mutations in non-small cell lung cancer: A meta-analysis. Mol. Diagn. Ther. *26*, 7–18. https://doi.org/10.1007/s40291-021-00563-1.

47. Ohashi, K., Maruvka, Y.E., Michor, F., and Pao, W. (2013). Epidermal growth factor receptor tyrosine kinase inhibitor–resistant disease. J. Clin. Oncol. *31*, 1070–1080. https://doi.org/10.1200/JCO.2012.43.3912.

48. Thatcher, N., Hirsch, F.R., Luft, A.V., Szczesna, A., Ciuleanu, T.E., Dediu, M., Ramlau, R., Galiulin, R.K., Bálint, B., Losonczy, G., et al. (2015). Necitumumab plus gemcitabine and cisplatin versus gemcitabine and cisplatin alone as first-line therapy in patients with stage IV squamous non-small-cell lung cancer (SQUIRE): An open-label, randomised, controlled phase 3 trial. Lancet Oncol. *16*, 763–774. https://doi.org/10.1016/S1470-2045(15)00021-2.

49. Paz-Ares, L., Mezger, J., Ciuleanu, T.E., Fischer, J.R., von Pawel, J., Provencio, M., Kazarnowicz, A., Losonczy, G., de Castro, G., Szczesna, A., et al. (2015). Necitumumab plus pemetrexed and cisplatin as first-line therapy in patients with stage IV non-squamous non-small-cell lung cancer (INSPIRE): an open-label, randomised, controlled phase 3 study. Lancet Oncol. *16*, 328–337. https://doi.org/10.1016/S1470-2045(15)70046-X.

50. Pirker, R., Pereira, J.R., Szczesna, A., von Pawel, J., Krzakowski, M., Ramlau, R., Vynnychenko, I., Park, K., Yu, C.-T., Ganul, V., et al. (2009). Cetuximab plus chemotherapy in patients with advanced non-small-cell lung cancer (FLEX): an open-label randomised phase III trial. Lancet *373*, 1525–1531. https://doi.org/10.1016/S0140-6736(09)60569-9.

51. Watanabe, S., Yoshioka, H., Sakai, H., Hotta, K., Takenoyama, M., Yamada, K., Sugawara, S., Takiguchi, Y., Hosomi, Y., Tomii, K., et al. (2019). Necitumumab plus gemcitabine and cisplatin versus gemcitabine and cisplatin alone as first-line treatment for stage IV squamous non-small cell lung cancer: A phase 1b and randomized, open-label, multicenter, phase 2 trial in Japan. Lung Cancer *129*, 55–62. https://doi.org/10.1016/j.lungcan.2019.01.005.

52. Cross, D.A.E., Ashton, S.E., Ghiorghiu, S., Eberlein, C., Nebhan, C.A., Spitzler, P.J., Orme, J.P., Finlay, M.R.V., Ward, R.A., Mellor, M.J., et al. (2014). AZD9291, an Irreversible EGFR TKI, Overcomes T790M-Mediated Resistance to EGFR Inhibitors in Lung Cancer. Cancer Discov. *4*, 1046–1061. https://doi.org/10.1158/2159-8290.CD-14-0337.

53. Chen, G., Kronenberger, P., Teugels, E., Umelo, I.A., and De Grève, J. (2012). Targeting the epidermal growth factor receptor in non-small cell lung cancer cells: the effect of combining RNA interference with tyrosine kinase inhibitors or cetuximab. BMC Med. *10*, 28. https://doi.org/10.1186/1741-7015-10-28.

54. Vander Mause, E.R., Atanackovic, D., Lim, C.S., and Luetkens, T. (2022). Roadmap to affinity-tuned antibodies for enhanced chimeric antigen receptor T cell function and selectivity. Trends Biotechnol. *40*, 875–890. https://doi.org/10.1016/j.tibtech.2021.12.009.

55. Park, S., Shevlin, E., Vedvyas, Y., Zaman, M., Park, S., Hsu, Y.-M.S., Min, I.M., and Jin, M.M. (2017). Micromolar affinity CAR T cells to ICAM-1 achieves rapid tumor elimination while avoiding systemic toxicity. Sci. Rep. *7*, 14366. https://doi.org/10.1038/s41598-017-14749-3.

56. Golden-Mason, L., Palmer, B.E., Kassam, N., Townshend-Bulson, L., Livingston, S., McMahon, B.J., Castelblanco, N., Kuchroo, V., Gretch, D.R., and Rosen, H.R. (2009). Negative immune regulator Tim-3 is overexpressed on T cells in hepatitis C virus infection and its blockade rescues dysfunctional CD4+ and CD8+ T cells. J. Virol. *83*, 9122–9130. https://doi.org/10.1128/JVI.00639-09.

57. Jones, R.B., Ndhlovu, L.C., Barbour, J.D., Sheth, P.M., Jha, A.R., Long, B.R., Wong, J.C., Satkunarajah, M., Schweneker, M., Chapman, J.M., et al. (2008). Tim-3 expression defines a novel population of dysfunctional T cells with highly elevated frequencies in progressive HIV-1 infection. J. Exp. Med. *205*, 2763–2779. https://doi.org/10.1084/jem.20081398.

58. Nebbia, G., Peppa, D., Schurich, A., Khanna, P., Singh, H.D., Cheng, Y., Rosenberg, W., Dusheiko, G., Gilson, R., ChinAleong, J., et al. (2012). Upregulation of the Tim-3/Galectin-9 pathway of T cell exhaustion in chronic hepatitis B virus infection. PLoS One *7*, e47648. https://doi.org/10.1371/journal.pone.0047648.

59. Yang, Z.-Z., Grote, D.M., Ziesmer, S.C., Niki, T., Hirashima, M., Novak, A.J., Witzig, T.E., and Ansell, S.M. (2012). IL-12 upregulates TIM-3 expression and induces T cell exhaustion in patients with follicular B cell non-Hodgkin lymphoma. J. Clin. Invest. *122*, 1271–1282. https://doi.org/10.1172/JCI59806.

60. Liu, J.-F., Wu, L., Yang, L.-L., Deng, W.-W., Mao, L., Wu, H., Zhang, W.-F., and Sun, Z.-J. (2018). Blockade of TIM3 relieves immunosuppression through reducing regulatory T cells in head and neck cancer. J. Exp. Clin. Cancer Res. *37*, 44. https://doi.org/10.1186/s13046-018-0713-7.

61. Dardalhon, V., Anderson, A.C., Karman, J., Apetoh, L., Chandwaskar, R., Lee, D.H., Cornejo, M., Nishi, N., Yamauchi, A., Quintana, F.J., et al. (2010). Tim-3/Galectin-9 pathway: Regulation of Th1 immunity through promotion of CD11b+Ly-6G+ myeloid cells. J. Immunol. *185*, 1383–1392. https://doi.org/10.4049/jimmunol.0903275.

62. Gorman, J.V., and Colgan, J.D. (2018). Acute stimulation generates Tim-3-expressing T helper type 1 CD4 T cells that persist *in vivo* and show enhanced effector function. Immunology *154*, 418–433. https://doi.org/10.1111/imm.12890.

63. Acharya, N., Sabatos-Peyton, C., and Anderson, A.C. (2020). Tim-3 finds its place in the cancer immunotherapy landscape. J. Immunother. Cancer *8*, e000911. https://doi.org/10.1136/jitc-2020-000911.

64. Du, W., Yang, M., Turner, A., Xu, C., Ferris, R.L., Huang, J., Kane, L.P., and Lu, B. (2017). TIM-3 as a target for cancer immunotherapy and mechanisms of action. Int. J. Mol. Sci. *18*, 645. https://doi.org/10.3390/ijms18030645.

65. Sabins, N.C., Chornoguz, O., Leander, K., Kaplan, F., Carter, R., Kinder, M., Bachman, K., Verona, R., Shen, S., Bhargava, V., and Santulli-Marotto, S. (2017). TIM-3 engagement promotes effector memory T cell differentiation of human antigen-specific CD8 T cells by activating mTORC1. J. Immunol. *199*, 4091–4102. https://doi.org/10.4049/jimmunol.1701030.

66. Kataoka, S., Manandhar, P., Lee, J., Workman, C.J., Banerjee, H., Szymczak-Workman, A.L., Kvorjak, M., Lohmueller, J., and Kane, L.P. (2021). The costimulatory activity of Tim-3 requires Akt and MAPK signaling and its recruitment to the immune synapse. Sci. Signal. *14*, eaba0717. https://doi.org/10.1126/scisignal.aba0717.

67. Talavera, A., Friemann, R., Gómez-Puerta, S., Martinez-Fleites, C., Garrido, G., Rabasa, A., López-Requena, A., Pupo, A., Johansen, R.F., Sánchez, O., et al. (2009). Nimotuzumab, an antitumor antibody that targets the epidermal growth factor receptor, blocks ligand binding while permitting the active receptor conformation. Cancer Res. *69*, 5851–5859. https://doi.org/10.1158/0008-5472.CAN-08-4518.

68. Goldstein, N.I., Prewett, M., Zuklys, K., Rockwell, P., and Mendelsohn, J. (1995). Biological efficacy of a chimeric antibody to the epidermal growth factor receptor in a human tumor xenograft model. Clin. Cancer Res. *1*, 1311–1318.

69. Butler, S.E., Brog, R.A., Chang, C.H., Sentman, C.L., Huang, Y.H., and Ackerman, M.E. (2022). Engineering a natural ligand-based CAR: Directed evolution of the stress-receptor NKp30. Cancer Immunol. Immunother. *71*, 165–176. https://doi.org/10.1007/s00262-021-02971-y.

70. Nakazawa, Y., Huye, L.E., Dotti, G., Foster, A.E., Vera, J.F., Manuri, P.R., June, C.H., Rooney, C.M., and Wilson, M.H. (2009). Optimization of the PiggyBac transposon system for the sustained genetic modification of human T lymphocytes. J. Immunother. *32*, 826–836. https://doi.org/10.1097/CJI.0b013e3181ad762b.

71. Morita, D., Nishio, N., Saito, S., Tanaka, M., Kawashima, N., Okuno, Y., Suzuki, S., Matsuda, K., Maeda, Y., Wilson, M.H., et al. (2018). Enhanced expression of anti-CD19 chimeric antigen receptor in piggyBac transposon-engineered T cells. Mol. Ther. Methods Clin. Dev. *8*, 131–140. https://doi.org/10.1016/j.omtm.2017.12.003.